scientific reports

Check for updates

OPEN

Heuristic assessment of choices for risk network control

Christopher Brissette[1,2,5], Xiang Niu[1,2,5], Chunheng Jiang[1,2], Jianxi Gao[1,2], Gyorgy Korniss[1,3] & Boleslaw K. Szymanski[1,2,3,4]✉

Data-driven risk networks describe many complex system dynamics arising in fields such as epidemiology and ecology. They lack explicit dynamics and have multiple sources of cost, both of which are beyond the current scope of traditional control theory. We construct the global economy risk network by combining the consensus of experts from the World Economic Forum with risk activation data to define its topology and interactions. Many of these risks, including extreme weather and drastic inflation, pose significant economic costs when active. We introduce a method for converting network interaction data into continuous dynamics to which we apply optimal control. We contribute the first method for constructing and controlling risk network dynamics based on empirically collected data. We simulate applying this method to control the spread of COVID-19 and show that the choice of risks through which the network is controlled has significant influence on both the cost of control and the total cost of keeping network stable. We additionally describe a heuristic for choosing the risks trough which the network is controlled, given a general risk network.

Network dynamics define a plethora of real world systems and describe the evolution of various spreading processes ranging from epidemiology to economic shocks. In recent years ideas from control theory have been adapted to network science with some success in understanding structural linear control of static networks[1–7], temporal networks[8–10], and multilayer networks[11]. Current work also focuses on networks with nonlinear dynamics[12,13], and systems described by time series data instead of dynamical equations[14,15]. Comparatively little work studies the evolution and control of risk networks where active risks incur additional cost to the controller beyond the cost of the input signal[16]. Risk networks consist of individual risk vertices and connections between them. Risk vertices within this network represent events which, if active, incur substantial costs[17]. The edges within this network then represent the propensity for active vertices to activate other neighboring risk vertices, incurring additional cost. In theory these costs may take many forms. For instance if we are considering the risk of deforestation, a cost we may care about is the loss of biodiversity. If we instead consider the risk of inflation, the cost may be financial. In general these costs can be difficult to quantify. In this paper, we assume we already have access to a preemptive quantitative assessment of costs associated with individual risks. This allows for a single metric to be used to quantify costs over many risks. Within the framework of an economic risk network, this "universal metric" for cost can be thought of simply as a currency which we relate all our incurred costs to. A differentiating factor of risk networks in the context of control is that the activity of a single risk has the capability of activating others in a potentially catastrophic cascade that makes component-oriented analysis of individual risks inadequate for understanding their consequences. To fully understand the prevailing risks around us, we must understand the ways in which those risks interact and the ways those interactions evolve yielding risk dynamics. Despite a large body of literature on risk management and mitigation[18–20], the fundamental questions of networked risk control are rarely discussed[16,21] as they are beyond the state of the art in both control engineering and network science.

Two problems facing the study of networked risk control are the need for explicit dynamics and optimizing over multiple cost types. The former arises from the fact most real-world dynamics are informally defined by data as opposed to the formal differential equations required for control theory. Additionally these risks are active or inactive and evolve as a Markov process depending on the network's current state. This poses a significant challenge to control theory, since applying theory from control analysis requires continuously defined dynamics for the risk variables.

[1]Network Science and Technology Center, Rensselaer Polytechnic Institute (RPI), Troy, NY 12180, USA. [2]Department of Computer Science, Rensselaer Polytechnic Institute (RPI), Troy, NY 12180, USA. [3]Department of Physics, Applied Physics, and Astronomy, Rensselaer Polytechnic Institute (RPI), Troy, NY 12180, USA. [4]Społeczna Akademia Nauk, Łódź, Poland. [5]These authors contributed equally: Christopher Brissette and Xiang Niu. ✉email: boleslaw.szymanski@gmail.com

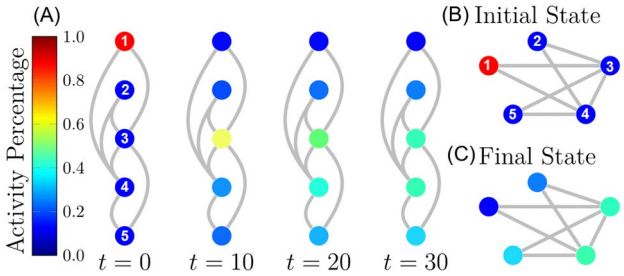

Figure 1. An example of continuous risk dynamics. Continuous risk dynamics simulated on a subnetwork from the World Economic Forum's Global Economy Risk Network. In order of the numerical labels in the figure, these nodes represent inflation, failure of climate change mitigation, interstate conflict, large scale migration, and cyberattacks. No control is applied and we can see that all nodes are inactive at the beginning of the simulation except for inflation. The activity from inflation can be seen to disperse over the network until all nodes are at a low level of activity at the end of the simulation.

Therefore, we introduce a continuous dynamical model describing how risk activation propagates through the underlying network. We model the network activity dynamics with an adaptation of a stochastic process that is based on an alternating renewal process[21–24] and is continuous. Instead of each risk transitioning to a discrete state indicating activity, we have the state of each node represent the expected value of risk i being active at time step $k+1$, $x_i(k+1)$ using the following model[21,25–27].

$$\vec{x}(k+1) = F[\vec{x}(k), \vec{p}_{int}, \vec{p}_{con}] + G[\vec{x}(k), \vec{p}_{ext}, E] + B\vec{u}(k) \tag{1}$$

Here $x_i(k)$ is the expected value of risk i at time step k. Both $F[\vec{x}(k), \vec{p}_{int}, \vec{p}_{con}]$ and $G[\vec{x}(k), \vec{p}_{ext}, E]$ are nonlinear dynamical functions depending on the state vector $\vec{x}(k)$. Here the probabilities $\vec{p}_{int}$, $\vec{p}_{ext}$, and $\vec{p}_{con}$ represent the internal and external probabilities of activation, and the probability nodes retain their state, respectively. Each of these probabilities is calculated according to a maximum likelihood estimation as discussed in previous work[25] as well as in the supplementary text. E is the adjacency matrix defining interactions between pairs of risks, and $B\vec{u}(k)$ defines our input control signals. Since the individual states $x_i(k)$ at the given time k vary in meaning for different applications, so too do the signal costs, $u_i(k)$. For example in the case of a Lotka Volterra network an individual control signal $u_i(k)$ may represent additional population added or removed at time k, where the state $x_i(k)$ represents the population of a given species at that time. Alternatively in a mechanical system $x_i(k)$ may represent quantities such as velocity, or force of moving components, while $u_i(k)$ represents energy applied to the system. In the case of the Lotka Volterra network the nonlinear dynamics $F[\vec{x}(k), \vec{p}_{int}, \vec{p}_{con}]$ and $G[\vec{x}(k), \vec{p}_{ext}, E]$ may instead represent the growth rate of a node's population based on its current population and its neighbor's populations respectively. Similarly, for a mechanical system the equations may represent the resistance of a component and the force being applied to it by other components respectively.

We note that while this model is convenient and provides accurate risk activity estimates, real risk networks are constantly evolving. Risks can be added to the network as they arise and they may also be removed due to factors such as governments and industries intervention. Consequently the underlying network changes and as such, the probabilities associated with each risk change to accommodate fluctuations in network interactions. This implies the risk network and its underlying dynamics should be regularly revisited and redefined. Using the above continuous equation, we apply an altered version of the linear-quadratic regulator to account for multiple cost types and ensure optimal control. We apply these methods to the annually published Global Economy Risk (GER) network from the World Economic Forum in order to obtain an interesting dynamic risk network and control it. The 2020 GER network can be seen in subfigure (A) of Fig. 2.

Globalization has provided extensive quality of life improvements for billions of people worldwide, including increased life expectancy, poverty reduction, and far reaching medical advances. Also due to globalization, risks are now more connected through the avenues of technology, business, and individuals than ever. As both the global economy and the technology defining our interactions become more connected, they are also becoming more vulnerable[16,17]. The annually reported global risk network from the World Economic Forum[16] currently represents the best understanding of the ways systemic risks are connected to each other. This network distills the immeasurably complex and constantly evolving network of global economic factors based on a consensus of expert opinions, and instead includes various transitions to catastrophic states such as unmanageable inflation[28], climate change[29], interstate conflict[30], involuntary migration[31], and large-scale cyber attacks[32], a subnetwork of these risks can be seen in Fig. 1.

While active, corresponding risks induce tremendous damages to resources, economies, and most importantly human lives. As examples consider the 2014 Ebola virus outbreak in Africa[33–35] and the 2008 financial meltdown triggered by a crisis in the subprime mortgage market[36–39]. Neither the viral outbreak nor the financial meltdown were confined to where they erupted nor limited to initially triggered risks, but continued to grow and affect other risks, often causing enormous losses. An even more contemporary example of networked risk dynamics comes from the 2019 breakout of COVID-19[40]. In response to the epidemic, nations around the world enacted a plethora of control measures to mitigate the virus's effects. While policies deviated between countries, control measures generally included the temporary closure of businesses, stimulus packages, and travel limitations. It is

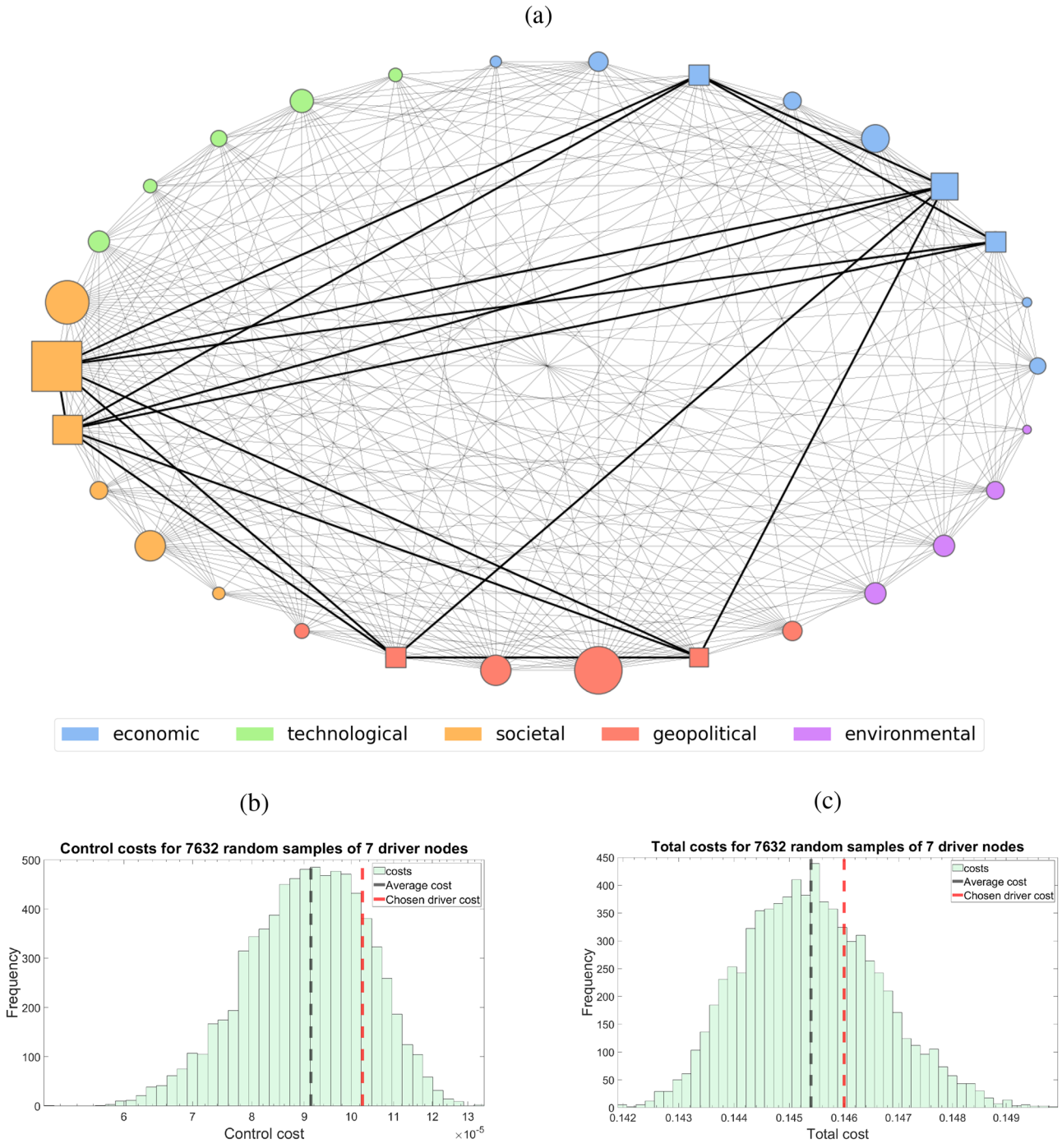

Figure 2. The cost of controlling infectious disease within the 2020 GER network. Incurred cost from LQR control for random samples of 7 driver nodes on the 2020 GER network with the "rapid and massive spread of infectious diseases" risk held constant at one. The network itself is dense and near regular with mean vertex degree of 18.27 and standard deviation of 4.60. We compare the 7 node costs with that of the nodal set consisting of deflation, failure of major financial institutions, unemployment, failure of national governance, failure of global governance, failure of urban planning, and profound social instability. In the above network we have highlighted the nodes within the 2020 GER network these drivers consist of by making them square. We can see that this driver set performs worse than an average randomly chosen driver set in both total cost and control cost.

still unknown what the long term fallout of COVID-19 will be, and understanding the risks associated with the disease is going to be important in addressing long term effects. According to the Global Bank, COVID-19 could lead to widespread school closings, increased dropout rates, and decreased development in human capital in

Europe and Central Asia[41]. In South America, the Caribbean, and South Africa the Global Bank suspects social unrest may arise due to food shortages related to COVID-19[41]. In addition to this analysis, the World Economic Forum also released a report on risks associated to COVID-19 based on the risks outlined in their yearly Global Risk Report[42]. They listed prolonged recession of the global economy, high levels of structural unemployment, tighter restriction on cross-border movement of people and goods, and economic collapse of emerging markets and developing economies as the most prevalent risks.

Results

Assessing control methods. To motivate the need for heuristic cost estimates in risk control, we examine the case of controlling the activity of COVID-19 within the 2020 network. We consider a set of seven control nodes within this network and use LQR control, an optimal control for linear dynamical system with quadratic cost[43], to attempt driving the dynamic global risk network towards inactivity in response to a perpetually active infectious disease. The nodal set consists of deflation, failure of major financial institutions, unemployment, failure of national governance, failure of global governance, failure of urban planning, and profound social instability. These nodes were chosen by the authors guided by a subjective assessment of government responses to COVID-19 and do not necessarily represent the true actions of governments. Instead this driver set is used to illustrate the effect that driver node choice has on control cost and total cost. The cost of control measures on this driver set is compared with the cost of controlling the network with randomly chosen sets of seven driver nodes. We could have chosen a driver set with a different number of control nodes, and one may expect these results to potentially change for different sizes of driver sets. However, we found that while individual costs change with different size driver sets, the overall distributions are similar. For this reason, we illustrate the total cost and control cost with a seven node driver set as it is representative of general cost behavior. The results of this simulation are demonstrated in Fig. 2. We find that the seven nodes chosen incur a relatively high cost among the sample; there are many more efficient sets of control nodes one could pick. This suggests that if government intervention indeed is enacted through these nodes, the policy decisions made in response to an infectious disease like COVID-19 would not be optimal among seven node driver sets. However, we reiterate that this driver set does not necessarily represent the control set chosen for actual government intervention. Instead, the problem of determining the set of driver nodes representing government intervention in the case of the COVID-19 pandemic realistically requires a multitude of expert opinions to establish. However, this driver set serves as a useful example of how total incurred cost can be used to evaluate driver node sets. It should additionally be noted that the costs associated with each risk are taken to be unit while in reality they would likely vary and require expert analysis to deduce. Because the costs are all unit, this method is giving us a qualitative understanding of how topologically important our chosen control set is within the dynamic risk network. This highlights the combinatorial nature of finding optimal risk driver sets and the need for heuristic assessment tools in choosing them. Unfortunately such heuristics are not widespread and the current understanding of risk assessment is often limited to individual, or narrow groups of risks[44–53]. The histograms in Fig. 2b,c come from simulations run on a random sample of 7632 7-node driver sets driving the dynamic global risk network. In these experiments the node associated with the spread of infectious disease was held constant and the control method being used is LQR control.

Nodal heuristics. We suggest two heuristics to help inform driver node choice when applying reactive and proactive control phases respectively on risk networks. Here, we denote reactive control as controlling the risks once they become active, and we do not need to take any action before it happens. We define proactive control as managing the risks before they become active, close to control for prevention. Call N_D the total number of driver nodes, N_{D_a} the number of driver nodes that are initially active, and N_{D_p} the number of driver nodes that are among the most active at the system's natural steady state $\vec{x}_s$. In Fig. 3, we see how N_{D_a} affects both the control cost and total cost in the reactive control phase. For the reactive phase we see a strong negative relation between the control cost and the total cost.

Each subfigure in Fig. 3 comes from a sample of 1200 driver node sets. Each driver set consists of 12 nodes. For subfigures (a) and (b) these 1200 diver node sets were divided into 12 groups of 100 random driver sets with each group having a consistent number of high activity driver nodes (N_{D_p}) ranging between 1 and 12 across the 12 groups. Subfigures (c) and (d) each consist of 1200 diver node sets were divided into 12 groups of 100 random driver sets with each group having a consistent number of initially active driver nodes (N_{D_a}) ranging between 1 and 12 across the 12 groups. We again note, as we did for Fig. 2, that there is nothing special about our choice of driver set size here. This is arbitrary and illustrates the trend of proactive and reactive control costs in relation to our defined heuristics. Similar behavior can be observed for many choices of driver set size.

Once the system has been driven to inactivity, the dynamics will continue to evolve towards the natural steady state of the system $\vec{x}_s$. To combat this, we use proactive control in which we apply a control signal to our driver nodes based on their activation probabilities at the natural steady state $\vec{x}_s$. The cost of this control phase depends on N_D just as the reactive phase did. We also find that the number of driver nodes with high activation probabilities at the natural steady state $\vec{x}_s$, N_{D_p} has a drastic effect on the control cost. In Fig. 3, we plot the control costs and total costs against each other for collections of driver nodes with different N_{D_p} in the proactive control phase. We can see that the trends are broadly similar to those seen in the reactive phase with respect to N_{D_a}. We see that a high number of N_{D_p} among our driver nodes generally reduces our total cost and increases our control cost. However, the control cost and total cost here have far smaller quartiles than in the reactive phase seen in Fig. 3.

It should be noted that applying this control to real-world networks is not a trivial problem in and of itself. In the case of the GER network, the control signal must be designed by experts and may take the form of strategies such as enacting legal policy, investing, or quarantining infections. In practice, it may require iterations of

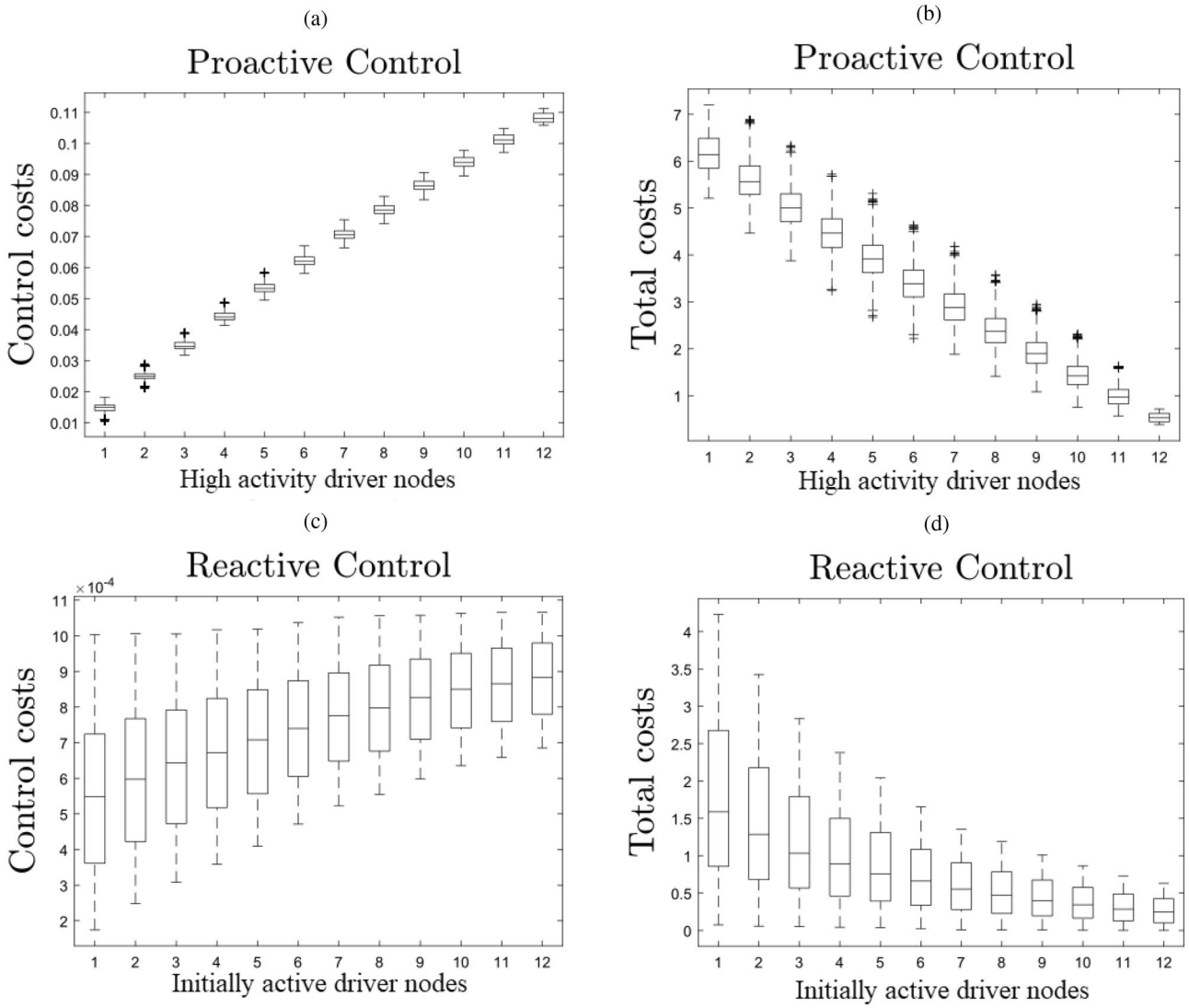

Figure 3. Heuristic assessment of node significance. We show the relationships between the number of "high impact" nodes in our control set N_{D_a} and N_{D_p} and the effects on costs incurred during the reactive and proactive control phases respectively. There were 12 total control nodes in all tests and for each associated N_{D_a} and N_{D_p} 100 driver node sets were sampled for a total of 1200 sampled driver sets in each subplot. In the proactive phase the network was controlled for 50 time steps, and in the reactive phase the network was controlled for 500 time steps. We can see that control costs went up with an increase in N_{D_a} or N_{D_p} in both the reactive and proactive control phases respectively. Alternatively we see the opposite trend in total costs. Total costs appear to decline far more with N_{D_p} in the proactive phase than they do with N_{D_a} in the reactive phase.

design to force risks towards inactivity, and in that time, the underlying network and probabilities defining its dynamics may change. Despite this, knowing which set of risks forms an optimal set of drivers is valuable in its own right and can minimize control costs.

Discussion

Networked risks provide a theoretical foundation for defining complex interactions between factors that are consistently prone to cascading failures. To avoid the damages of inevitable steady states that arise from the interactions of these networks, we require an optimal method to them. The dynamics resulting from these networks are difficult to analytically define for use in control theory since they must be constructed from probabilities and extensive data collection. Our method presents a pipeline for constructing dynamic risk networks from extensive data and how to control them. This requires using a massive amount of collected data and applying maximum likelihood estimation in order to predict transition probabilities. Using these transition probabilities, we can construct continuous dynamics from the alternating renewal process[22] that defines the network's underlying discrete dynamics. In these new continuous dynamics, the state of each node represents its probability of activity over the current time step as opposed to the initially defined discrete dynamics. These continuous dynamics allow for the application of control methods for driving the system into inactivity. We adapt LQR to account for

risk networks in which control cost and risk activity cost are simultaneously considered. We also show that by altering the control strategy before and after driving the network to inactivity we can drastically reduce the total cost of controlling the system.

The tools proposed in this paper are very general and widely applicable. It should be noted that a trade-off between proactive and reactive control arises not only in risk networks but in any system in which the desired final state of control is not stable. Most of the control designs for such systems make a salient assumption that the cost of the system being out of the desired final state is negligible. Certainly, there are other systems than risk networks, in which this assumption is not true. Our approach to control such systems in two phases, reactive and proactive, can be applied to such cases. Hence the usefulness of our approach reaches beyond risk networks.

We note that this model requires consistent reevaluation from experts. Both the connectivity and the weighting of the links in the dynamic risk network are subject to change as experts reevaluate and add new risks. Additionally the cost matrices used in our model are subject to change with expert evaluation as well. Furthermore, applying the linear quadratic regular as an explicit control method to the dynamic global risk network is difficult in practice. The control signal being added to nodes in our control set varies over many professional domains and would realistically require the fine tuning of many distinct policy decisions. For this reason, in many real world applications we suggest that this method be used as a heuristic for evaluating comparative costs between driver node sets as opposed to an explicit method for generating real-world control strategies.

Methods

Controlling risk networks. When applying control theory to nonlinear problems, we require a linearization of the underlying nonlinear dynamics. Assume that when uncontrolled, the system in equation (2) approaches a natural steady state $\vec{x}_s$. Also assume $f_x = F + G$ and $A = \frac{\partial f_x}{\partial \vec{x}}|_{\vec{x}=\vec{x}_s,\vec{u}=\vec{u}_s}$ is the adjacency matrix defining the underlying probability of activation between links. Then we linearize (1) as follows.

$$\Delta\vec{x}(k+1) \approx A\Delta\vec{x}(k) + B\Delta\vec{u}(k) \tag{2}$$

Here $\Delta\vec{x}(k) = \vec{x}(k) - \vec{x}_s$ and $\Delta\vec{u}(k) = \vec{u}(k) - \vec{u}_s$. If the linearized system (3) is locally controllable along a specific trajectory then the associated non-linear system is controllable along the same trajectory[54]. Therefore the linearized system is sufficient for several parts of control analysis including determination of driver nodes and determination of instantaneous optimal control. In traditional control, the control energy after τ time steps is expressed as a sum over our control signal at each time step given by $J_\epsilon = \sum_{k=0}^{\tau-1} ||\vec{u}(k)||^2$. J_ϵ depends only on the control signal, whereas we require a cost function additionally depending on risk activity. For this purpose, we alter the cost function of the linear quadratic regulator to obtain the following control cost which includes the cost of active risks[43].

$$J_t(Q_f, Q, R) = \vec{x}^T(\tau)Q_f\vec{x}(\tau) + \sum_{k=k_0}^{\tau-1}[\vec{x}^T(k)Q\vec{x}(k) + \vec{u}^T(k)R\vec{u}(k)] \tag{3}$$

Here Q_f denotes the cost matrix at the final state, Q is the cost matrix for intermediate states, and R is the cost matrix for our control signals. Examining this equation we see that the right most term is a sum over the costs associated with the state of each risk and the control cost being applied to each risk. For our tests we assume all of these matrices to be the identity for simplicity. As such, we have expressed the cost of controlling our risk network in a form where we may apply an optimal control strategy to reduce the overall incurred cost. Further information about optimal control and linear quadratic regulators can be found in the supplementary text.

In the case of networked risks, system dynamics have a natural steady state we will refer to as $\vec{x}_s$. This is the state that the system will approach in the absence of a control signal. Because of this, when trying to drive the entire network towards an alternate state $\vec{x}_* \neq \vec{x}_s$ it is necessary to continuously apply a control signal. Therefore, we introduce a distinction between reactive and proactive control. It is important to note that this is common in risk reduction literature[18], however it lacks theoretical or heuristic tools for assessment.

Data availability

All Matlab code and associated data may be found and downloaded at the following link, https://drive.google.com/drive/folders/1sHj4m_M8O4jAvBNlCs6aCnBbkqJwzboU?usp=sharing.

Received: 9 December 2020; Accepted: 28 February 2021
Published online: 07 April 2021

References

1. Liu, Y.-Y., Slotine, J.-J. & Barabási, A.-L. Controllability of complex networks. *Nature* **473**, 167 (2011).
2. Yan, G. *et al.* Spectrum of controlling and observing complex networks. *Nat. Phys.* **11**, 779 (2015).
3. Yan, G. *et al.* Network control principles predict neuron function in the *Caenorhabditis elegans* connectome. *Nature* **550**, 519 (2017).
4. Nepusz, T. & Vicsek, T. Controlling edge dynamics in complex networks. *Nat. Phys.* **8**, 568 (2012).
5. Ruths, J. & Ruths, D. Control profiles of complex networks. *Science* **343**, 1373–1376 (2014).
6. Gao, J., Liu, Y.-Y., D'souza, R. M. & Barabási, A.-L. Target control of complex networks. *Nat. Commun.* **5**, 5415 (2014).
7. Liu, X., Pan, L., Stanley, H. E. & Gao, J. Controllability of giant connected components in a directed network. *Phys. Rev. E* **95**, 042318 (2017).
8. Li, A., Cornelius, S. P., Liu, Y.-Y., Wang, L. & Barabási, A.-L. The fundamental advantages of temporal networks. *Science* **358**, 1042–1046 (2017).

9. Pósfai, M. & Hövel, P. Structural controllability of temporal networks. *New J. Phys.* **16**, 123055 (2014).
10. Paranjape, A., Benson, A. R. & Leskovec, J. Motifs in temporal networks. In *Proceedings of the Tenth ACM International Conference on Web Search and Data Mining*, 601–610 (ACM, 2017).
11. Pósfai, M., Gao, J., Cornelius, S. P., Barabási, A.-L. & D'Souza, R. M. Controllability of multiplex, multi-time-scale networks. *Phys. Rev. E* **94**, 032316 (2016).
12. Zañudo, J. G. T., Yang, G. & Albert, R. Structure-based control of complex networks with nonlinear dynamics. *Proc. Natl. Acad. Sci.* **114**, 7234–7239 (2017).
13. Cornelius, S. P., Kath, W. L. & Motter, A. E. Realistic control of network dynamics. *Nat. Commun.* **4**, 1942 (2013).
14. Toroczkai, Z. Geometric method for stabilizing unstable periodic orbits. *Phys. Lett. A* **190**, 71–78 (1994).
15. Sass, B. & Toroczkai, Z. Continuous extension of the geometric control method. *J. Phys. A: Math. Gen.* **29**, 3545 (1996).
16. Helbing, D. Globally networked risks and how to respond. *Nature* **497**, 51 (2013).
17. World Economic Forum Global Risks Report. http://www3.weforum.org/docs/WEF_Global_Risks_Report_2020.pdf (2020). Accessed: 2020-26-8.
18. Tait, J. & Levidow, L. Proactive and reactive approaches to risk regulation: the case of biotechnology. *Futures* **24**, 219–231 (1992).
19. Erisman, J. W., Brasseur, G., Ciais, P., van Eekeren, N. & Theis, T. L. Global change: put people at the centre of global risk management. *Nat. News* **519**, 151 (2015).
20. WHO Ebola Response Team. After Ebola in West Africa—unpredictable risks, preventable epidemics. *N. Engl. J. Med.* **375**, 587–596 (2016).
21. Szymanski, B. K., Lin, X., Asztalos, A. & Sreenivasan, S. Failure dynamics of the global risk network. *Sci. Rep.* **5**, 10998 (2015).
22. Cox, D. & Miller, H. *The Theory of Stochastic Processes* (Methuen, London, 1965).
23. Yao, K. & Li, X. Uncertain alternating renewal process and its application. *IEEE Trans. Fuzzy Syst.* **20**, 1154–1160 (2012).
24. Majdandzic, A. *et al.* Spontaneous recovery in dynamical networks. *Nat. Phys.* **10**, 34–38 (2014).
25. Lin, X., Moussawi, A., Korniss, G., Bakdash, J. Z. & Szymanski, B. K. Limits of risk predictability in a cascading alternating renewal process model. *Sci. Rep.* **7**, 6699 (2017).
26. Niu, X. *et al.* Evolution of the global risk network mean-field stability point. In *International Workshop on Complex Networks and their Applications*, 1124–1134 (Springer, 2017).
27. Niu, X., Moussawi, A., Korniss, G. & Szymanski, B. K. Evolution of threats in the global risk network. *Appl. Netw. Sci.* **3**, 24 (2018).
28. Pindiriri, C. Monetary reforms and inflation dynamics in Zimbabwe. *Int. Res. J. Finance Econ.* **90**, 207–222 (2012).
29. Lobell, D. B. *et al.* Prioritizing climate change adaptation needs for food security in 2030. *Science* **319**, 607–610 (2008).
30. Lee Ray, J. Explaining interstate conflict and war: What should be controlled for?. *Confl. Manag. Peace Sci.* **20**, 1–31 (2003).
31. McGregor, J. Climate change and involuntary migration: implications for food security. *Food Policy* **19**, 120–132 (1994).
32. Cashell, B., Jackson, W. D., Jickling, M. & Webel, B. The economic impact of cyber-attacks. Congressional Research Service Documents, CRS RL32331 (Washington DC) (2004).
33. Piot, P., Muyembe, J.-J. & Edmunds, W. J. Ebola in West Africa: from disease outbreak to humanitarian crisis. *Lancet Infect. Dis* **14**, 1034–1035 (2014).
34. World Health Organization. World Health Organization. http://www.who.int/ebola/ (2018). Accessed: 2018-10-15.
35. Dellicour, S. *et al.* Phylodynamic assessment of intervention strategies for the West African Ebola virus outbreak. *Nat. Commun.* **9**, 2222 (2018).
36. Morris, S. & Shin, H. S. Financial regulation in a system context. *Brook. Pap. Econ. Act.* **2008**, 229–274 (2008).
37. Reinhart, C. M. & Rogoff, K. S. Is the 2007 US sub-prime financial crisis so different? An international historical comparison. *Am. Econ. Rev.* **98**, 339–44 (2008).
38. Ivashina, V. & Scharfstein, D. Bank lending during the financial crisis of 2008. *J. Financ. Econ.* **97**, 319–338 (2010).
39. Battiston, S. *et al.* Complexity theory and financial regulation. *Science* **351**, 818–819 (2016).
40. Zhong, L., Diagne, M., Wang, W. & Gao, J. Country distancing reveals the effectiveness of travel restrictions during covid-19. *medRxiv* (2020).
41. Pandemic,Recession: The Global Economy in Crisis. https://openknowledge.worldbank.org/bitstream/handle/10986/33748/9781464815539.pdf (2020). Accessed: 2020-07-28.
42. COVID-19 Risks Outlook A Preliminary Mapping and Its Implications. http://www3.weforum.org/docs/WEF_COVID_19_Risks_Outlook_Special_Edition_Pages.pdf (2020). Accessed: 2020-07-28.
43. Lewis, F. L., Vrabie, D. & Syrmos, V. L. *Optimal Control* (Wiley, Hoboken, 2012).
44. Winsemius, H. C. *et al.* Global drivers of future river flood risk. *Nat. Clim. Change* **6**, 381 (2016).
45. O'Neill, B. C. *et al.* IPCC reasons for concern regarding climate change risks. *Nat. Clim. Change* **7**, 28 (2017).
46. Hoekstra, A. Y. Water scarcity challenges to business. *Nat. Clim. Change* **4**, 318 (2014).
47. Wada, Y., Gleeson, T. & Esnault, L. Wedge approach to water stress. *Nat. Geosci.* **7**, 615 (2014).
48. Manning, M. R. *et al.* Misrepresentation of the IPCC CO2 emission scenarios. *Nat. Geosci.* **3**, 376 (2010).
49. Vörösmarty, C., Hoekstra, A., Bunn, S., Conway, D. & Gupta, J. What scale for water governance. *Science* **349**, 478–479 (2015).
50. Pekel, J.-F., Cottam, A., Gorelick, N. & Belward, A. S. High-resolution mapping of global surface water and its long-term changes. *Nature* **540**, 418 (2016).
51. Mekonnen, M. M. & Hoekstra, A. Y. Four billion people facing severe water scarcity. *Sci. Adv.* **2**, e1500323 (2016).
52. Maynard, A. D. The (nano) entrepreneur's dilemma. *Nat. Nanotechnol.* **10**, 199 (2015).
53. Liang, B. A. & Mackey, T. K. Sexual medicine: online risks to health—the problem of counterfeit drugs. *Nat. Rev. Urol.* **9**, 480 (2012).
54. Slotine, J.-J.E. & Li, W. *Applied Nonlinear Control* Vol. 199 (Prentice Hall, Englewood Cliffs, 1991).

Acknowledgements

This work was partially supported by the Army Research Laboratory under NS CTA Agreement W911NF-09-2-0053, the Army Research Office Grant W911NF-16-1-05241, and the Office of Naval Research Grant N00014-15-1-2640.

Author contributions

G.K., X.N., and *B.K.S. conducted research on dynamics of global risk networks. J.G., X.N., and *B.K.S. conducted research on control of data driven networks. C.B., J.G., and *B.K.S. conducted research on pandemic control. C.B., C.J., and X.N. designed software, ran computer experiments, and collected data. C.B. wrote the first draft of the manuscript. All authors analyzed results, edited and approved the manuscript.

Additional information

Supplementary Information The online version contains supplementary material available at https://doi.org/10.1038/s41598-021-85432-x.

Correspondence and requests for materials should be addressed to B.K.S.